Proceedings Paper:
Dogan, H. orcid.org/0000-0002-6523-7290, Sims, N.D. orcid.org/0000-0002-6292-6736 and Wagg, D.J. orcid.org/0000-0002-7266-2105 (2020) The effects of parasitic mass on the performance of inerter-based dynamic vibration absorbers. In: Papadrakakis, M., Fragiadakis, M. and Papadimitriou, C., (eds.) EURODYN 2020: Proceedings of the XI International Conference on Structural Dynamics. EURODYN 2020: XI International Conference on Structural Dynamics, 23-26 Nov 2020, Athens, Greece. European Association for Structural Dynamics (EASD) , pp. 1545-1555. ISBN 9786188507227

10.47964/1120.9125.19507

EURODYN 2020
XI International Conference on Structural Dynamics
M. Papadrakakis, M. Fragiadakis, C. Papadimitriou (eds.)
Athens, Greece, 22—24 June 2020

THE EFFECTS OF PARASITIC MASS ON THE PERFORMANCE OF INERTER-BASED DYNAMIC VIBRATION ABSORBERS

Hakan Dogan, Neil D. Sims, and David J. Wagg

University of Sheffield
Department of Mechanical Engineering, University of Sheffield, S1 3JD, UK
e-mail: {hdogan1, n.sims, david.wagg}@sheffield.ac.uk

Keywords: Inerter, Parasitic mass, Inerter-based dynamic vibration absorber.

Abstract. *This study investigates the effects of parasitic mass on the performance of inerter-based dynamic vibration absorbers (IDVAs). IDVAs have been increasingly employed to suppress vibrations in applications of civil engineering structures and vehicle suspension systems. While the masses of the components in a traditional dynamic vibration absorber can be easily compensated for due to its simple layout, the masses of the components in an IDVA can act as parasitic mass and might affect the performance of IDVAs. This can lead to the loss of benefits which is provided by the IDVAs. The negative effect of a parasitic mass in an IDVA can be observed in applications which have smaller inertance values. In such cases, it is important to consider masses of the components while selecting optimal parameters to maximize the performance improvement which can be obtained by an IDVA. In this study, a milling operation is modelled and its machining stability is increased by utilizing an IDVA. The negative effect of a parasitic mass on the performance is shown, and the performance improvement is regained by considering the parasitic mass in the tuning strategy.*

1 INTRODUCTION

Tuned mass dampers (TMDs) have been successfully employed to suppress vibration since the concept was introduced by Frahm [1] in the early 20th century. The device which was proposed by Frahm, the so-called dynamic vibration absorber (DVA), consists of an auxiliary mass and a spring. It targets the natural frequency of the system that is required to be controlled. Although it can successfully suppress vibrations at the resonance frequency, it allows high amplitude vibrations near the resonance frequency. This drawback of the DVA was modified by adding a viscous damper in the work of Den Hartog [2]. The resulting tuned mass damper (TMD) has the capability to suppress vibration at a wider range of frequencies. The tuning methodology was also developed by Den Hartog [2] using the fixed-points-theory.

To increase the performance of the TMD, a relative-acceleration-dependent-inertial element in conjunction with a spring and a damper, was studied by Kuroda [3]. This concept was analysed by many authors, for example Saito [4] investigated how it could be used to control seismic response of the structures. Similarly, the inerter, which was first introduced by Smith [5] by using the force-current analogy between mechanical and electrical networks, applies forces proportional to the relative acceleration between the two terminals. There are three types of inerter which have been mostly studied in the literature: the ball-screw inerter [6], the rack and pinion inerter [5, 6], and the fluid inerter [7]. Recently, the frictionless mechanical inerter that consists of a disc as flywheel and the living-hinges was presented to eliminate the friction that is caused by gears or ball-screw interaction [8]. Inerter-based vibration absorbers have been studied to improve the vibration performance of the system in vehicle suspensions [9, 10], civil engineering applications [11, 12, 13], landing-gear systems [14] and machining applications [15, 16].

Tuning parameters of the components of the inerter-based device plays an important role in the their vibration suppression performance. Lazar et al. [11] proposed a tuning strategy based on Den Hartog's fixed-points-theory for a tuned inerter damper (TID). Hu and Chen [17] used a direct search method to obtain design parameters of inerter-based dynamic vibration absorbers (IDVAs) for H_2 and H_∞ optimisations. Shen et al. [18] utilized a genetic algorithm to find the optimal parameters for the vibration suppression of the vehicle body controlled by an IDVA. Barredo et al. [19] presented an analytical methodology to obtain close-form solutions of three inerter-based configurations for an undamped primary system. Generally, the mass of the inerter is neglected in the mathematical model of the system during the process of finding the optimal parameters. This is because the inertance value of the inerter is generally very large compared to the mass of the inerter. However, for instance, the optimal inertance value for a small-primary-mass application can be small so that the mass of the inerter cannot be constructed small enough to neglect. In such cases, the mass of the inerter can act as a parasitic mass and lower the vibration suppression performance of the system being controlled.

This study investigates the effect of the parasitic mass caused by the mass of the components of the inerter. The novelty is that this parasitic mass is considered in the mathematical model and included in the evaluation of the performance of an IDVA. The effect of the parasitic mass is shown with two scenarios: the vibration suppression of a structure and the chatter stability of a milling operation. The effects of the parasitic mass are evaluated in the discussion section and finally the conclusions are presented.

2 PARASITIC MASS DUE TO AN INERTER

The inerter is a mechanical device which generates equal and opposite inertial forces proportional to the relative acceleration applied at the two nodes [5]. An ideal inerter can be represented as shown in Figure 1(a) and the schematic view of a physical realisation of the inerter [8] can be seen in Figure 1(b). The inerter in Figure 1(b) consists of a disc, which is the flywheel, in the middle and two legs that are the nodes of the inerter. The connections between the legs and the flywheel can be established by living-hinges to eliminate the friction and the backlash or by simple pin joints. The inertance of the inerter can be calculated as [8]

$$b = \frac{I_{disc}}{l_a^2} \tag{1}$$

where I_{disc} is the moment of inertia of the disc and l_a^2 is the distance between the points where the two legs are connected to the flywheel disc. Hence the inertial force generated by the inerter is

$$F_{inerter} = b(\ddot{x}_2 - \ddot{x}_1) \tag{2}$$

Equation 1 gives the inertance of an ideal inerter using a disc as a flywheel in Figure 1(b). The inertance values for the different types of inerters are calculated in a similar manner [5, 7, 20]. Once again, these inertance values are for an ideal inerter so the masses of the components of the inerter (e.g. the mass of the housing in a ballscrew inerter, the mass of the rack in a rack and pinion inerter or the mass of the legs in an inerter as shown in Figure 1(b)) are neglected. This is because the inertia of these parts is typically small compared with the inertance of the inerter device. Intrinsically, an inerter works as a kind of an inertia amplifier in most cases. Thus, it has higher inertance and the inertial increment in the device allows one to neglect the inertia of those which do not contribute this increment.

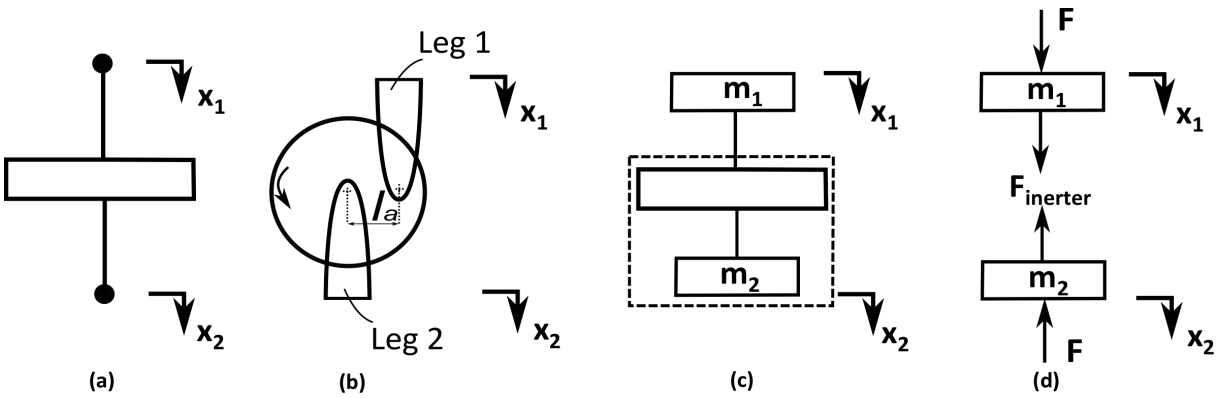

Figure 1: (a) Mathematical model of an ideal inerter, (b) schematic view of a small-scale mechanical inerter, (c) mathematical model of the inerter including the masses of legs and disc (the inertance value of the inerter involves only the rotational inertia of the disc.), (d) free body diagram of the inerter.

If the inertia of all components is considered, the mathematical model of an inerter becomes as shown in Figure 1(c) rather than in Figure 1(a). Leg 2 in Figure 1(b) is connected to the centre of the mass of the disc. The living-hinges or the pin joints, which are considered in the realisation, allow only rotational motion so that the disc and Leg 2 can be considered as rigidly connected in the translation motion. Hence, m_2 is the sum of the mass of the disc and the mass of Leg 2 while m_1 is equal to the mass of the Leg 1. The inertia of the inerter in Figure 1(c)

involves only the rotational inertia of the disc as expressed in Equation 1. Two inertial elements (m_1 and m_2) appear on the two nodes of the inerter in Figure 1(d) and induce the forces $m_1\ddot{x}_1$ and $m_2\ddot{x}_2$.

If the node with the inertial element is mounted on a spring or a damper, the inertial element (mass) acts as a parasitic mass between the inerter and the spring or the damper. The parasitic mass can be neglected in two cases where (1) the node with the inertial element has a ground connection or is mounted to another mass, and (2) the inertance value of the inerter is too large compared with the inertial element. Otherwise, the parasitic mass must be considered in the calculations.

3 MATHEMATICAL MODEL WITH A PARASITIC MASS

A tuned inerter damper consists of a spring which is connected to a damper in parallel, and an inerter which is in a series connection with the spring and the damper. Since one of the terminals of the inerter is connected to the spring and the damper, the parasitic mass can be observed in this configuration. The mathematical model of the TID with an ideal inerter is represented in Figure 2.

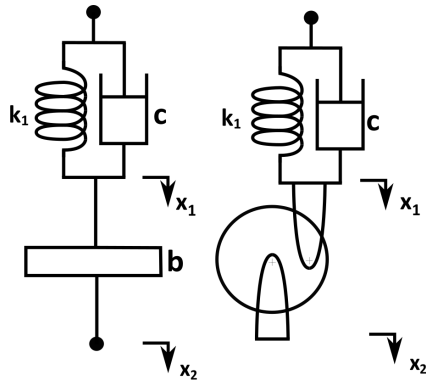

Figure 2: Mathematical model of a tuned mass damper with an ideal inerter, where the masses of the body of the inerter and the legs are neglected.

The TID can be employed to suppress a single-degree-of-freedom system which is under an excitation. The TID in a series connection with a spring, which is an IDVA, can be mounted to the primary system with a spring in series connection as shown in Figure 3(a). In reality, depending on the location of the inerter, either of the mathematical models in Figures 3(b) and 3(c) is a better representation than the model in Figure 2 due to the parasitic mass as discussed in the previous section. The upper nodes in Figures 3(b) and 3(c) are connected to the primary mass in Figure 3(a), and the bottom nodes are fixed to the auxiliary mass. Therefore, the inertial elements on these nodes can be neglected as the inertial element can be simply added to the mass which the nodes are connected to. Both of the mathematical models in Figure 3(b) and Figure 3(c) involve the parasitic mass m_p owing to the mass of the inerter as well as the masses of the spring and damper.

The location of the inerter, whether it is located in the bottom or the upper side, is not important if there is no parasitic mass between the inerter, and the spring and the damper. It matters if there is a parasitic mass since the equations of motion of the whole system will differ. The equations of motion for Figure 3(b), where the inerter is connected to the auxiliary mass (This layout is named in this paper as $icma$), can be written as

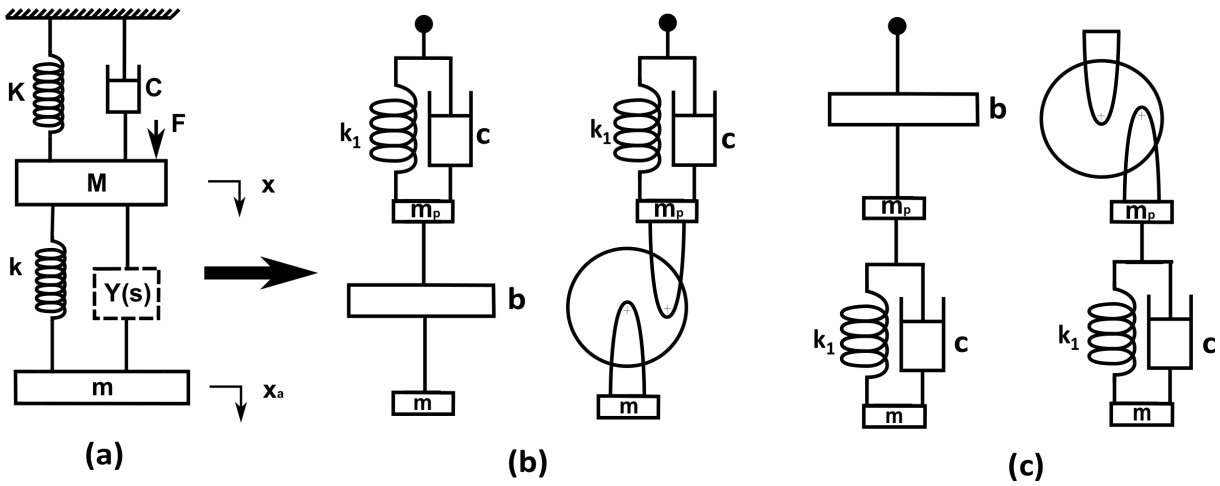

Figure 3: (a) Mathematical model of a structure controlled by an IDVA. Y(s) represents the impedance of the configuration in series connection with a spring. (b) Mathematical model of the case where the inerter is connected to the auxiliary mass,m (the $icma$). (c) Mathematical model of the case where the inerter is connected to the primary mass,M (the $icmp$).

$$\begin{aligned} M\ddot{x} + (C+c)\dot{x} + (K+k_1)x - c\dot{x_p} - k_1 x_p &= F \\ -c\dot{x} - k_1 x + (m_p+b)\ddot{x_p} + c\dot{x_p} + k_1 x_p - b\ddot{x_a} &= 0 \\ -b\ddot{x_p} + (m_a+b)\ddot{x_a} &= 0 \end{aligned} \tag{3}$$

where x, x_p and x_a are the displacements of the primary, parasitic and auxiliary masses, respectively. The equations of motion for Figure 3(c), where the inerter is connected to the primary mass (this layout is named in this paper as $icmp$), can be written as

$$\begin{aligned} (M+b)\ddot{x} + C\dot{x} + Kx - b\ddot{x_p} &= F \\ -b\ddot{x} + (m_p+b)\ddot{x_p} + c\dot{x_p} + k_1 x_p - c\dot{x_a} - k_1 x_a &= 0 \\ -c\dot{x_p} - k_1 x_p + m_a\ddot{x_a} + c\dot{x_a} + kx_a &= 0 \end{aligned} \tag{4}$$

The inertia of the parasitic mass is always added to the inertance of the inerter as seen Equations 3 and 4. Hence, the mass of the inerter is neglected if the inertance is too high.

4 THE EFFECT OF THE PARASITIC MASS

The system considered in this study to investigate the effect of the parasitic mass on the performance of a tuned inerter damper is depicted in Figure 3(a). A TID in series with a spring is mounted to the primary mass in a single-degree-of-freedom system to examine three mathematical models: No parasitic mass, the $icma$, and the $icmp$ cases. The effect of the parasitic mass on the vibration and chatter suppression performances is analysed.

4.1 Vibration Suppression Case

The study of Hu and Chen [17] has already shown that the inerter-based configuration which is presented in this work improved the vibration suppression performance of an undamped system. Therefore, a parasitic mass in this configuration can be considered to observe the effect

of the parasitic mass. The system with a parasitic mass is governed by either Equations 3 or 4, depending on the position of the inerter. The frequency response function (FRF) is given in the form as

$$H_i(j\omega) = \frac{X(jw)}{F(jw)} = \frac{R_{Ni} + jI_{Ni}}{R_{Di} + jI_{Di}}, \quad i = 1, 2, 3 \tag{5}$$

where $i = 1$, $i = 2$ and $i = 3$ represent for three mathematical models: No parasitic mass, the $icma$ and the $icmp$ cases, respectively.

The primary mass and the natural frequency of the primary system were taken as $M = 5\ kg$ and $f_n = 200\ Hz$. The primary system considered an undamped system and thus, $\zeta_{primary} = 0$. In order to obtain optimal design parameters (k, k_1, c and b), Self-adaptive Differential Evolution (SaDE) algorithm [21] can be utilized as a numerical optimisation method. The objective function for a constant mass ratio ($\mu = m/M$) can be written as

$$min_{k,k_1,c,b}\left(max_{\omega}\left(|H_i(j\omega)|\right)\right), i = 1, 2, 3 \tag{6}$$

since the minimisation of the maximum absolute value of the FRF is desired.

The optimal design parameters were found for mass ratio $\mu = 0.1$ and the case with no parasitic mass. The optimal inertance value for the case with no parasitic mass was found $b = 0.0965\ kg$. 5% and 10% of the inertance value, which are $4.8\ g$ and $9.6\ g$, were added as the parasitic mass to examine the two cases. For 5% parasitic mass, the optimal design parameters was obtained. The optimal parameters are given in Table 1 and the results are demonstrated in Figures 4 and 5.

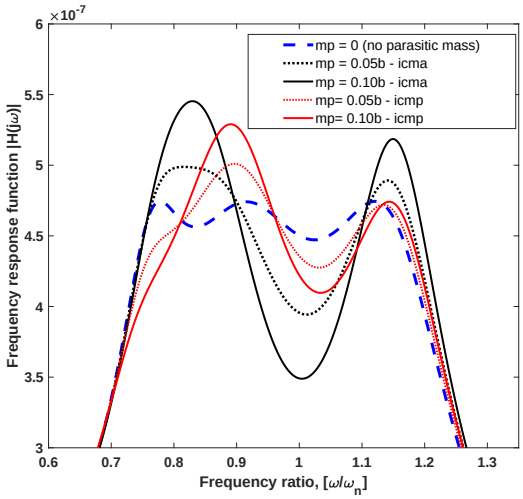

Figure 4: The magnitude of the FRF obtained from three cases: No parasitic mass, the $icma$ and the $icmp$ for parasitic masses of 5% and 10% of the optimal inertance value.

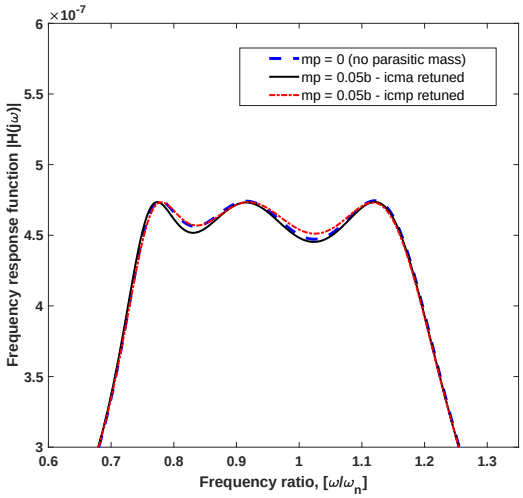

Figure 5: The magnitude of the FRF after retuning the optimal parameters considering a parasitic mass of 5% of the optimal inertance value.

The results show that both of the parasitic masses increased the amplitude of the vibration. The higher parasitic mass added caused the higher amplitude as shown in Figure 4. The $4.8\ g$ parasitic masses increased the amplitude of the displacement by 4.84% for the $icma$ and 5.39% for the $icmp$ After retuning the parameters for $4.82\ g$ parasitic mass, Figure 5 shows that the

Configurations	$m_p\ [g]$	$k\ [kN/m]$	$k_1\ [kN/m]$	$b\ [kg]$	$c\ [Ns/m]$
No parasitic mass	0	712.4	11.7	0.0965	60.3
$icma$	4.8	709.0	121.5	0.0999	64.5
$icmp$	4.8	721.5	115.2	0.0950	63.6

Table 1: Optimal design parameters obtained to suppress the vibrations in Figure 3(a) for $\mu = 0.1$.

same level of vibration suppression was provided again. Furthermore, the amplitude of the displacement was decreased by 0.2% compared to the case with no parasitic mass.

5 CASE STUDY ON MACHINING STABILITY

One potential application of inerters is in the suppression of vibrations during machining [15, 16]. Here, alternative methods for passive vibration control have already been proposed [22], and it has been shown that such approaches can improve the productivity by avoiding the onset of unstable self-excited vibrations known as chatter.

Consequently, this section provides a brief numerical case study to demonstrate how inerter systems can be used to suppress chatter. For simplicity, a turning configuration is chosen in order to demonstrate the concept without recourse to detailed theoretical analysis.

The mechanism which leads to regenerative chatter for a turning operation is briefly given here and explained comprehensively in [23, 24]. The cutting force which is applied to a flexible cutting tool leads to the waviness on the surface of the workpiece as shown in Figure 6. The phase difference (ε) between the waviness of the previous and the current cuts which are induced by the previous and the current displacements of the cutting tool, $y(t)$ and $y(t-T)$, causes a change in the instantaneous chip thickness. This variation in the instantaneous chip thickness induces a variation in the cutting force as the cutting force is proportional to the cross-sectional area of the chip and thus, the chip thickness. The variation in the cutting force leads to the waviness on the surface of the workpiece again. This regenerative mechanism can cause instability in the cutting operation.

The delay term T in the displacement in the previous cut $y(t-T)$ is introduced by the spindle rotation. Hence, for a machinist, two parameters which define the cutting force and accordingly a stable cut in a machining operation are the depth of cut and the spindle speed. The chatter stability of a machining process is generally evaluated over stability lobe diagrams (SLDs), which give the stability boundary in terms of the depth of cut for each spindle speed. The results for this study case will be presented as SLDs.

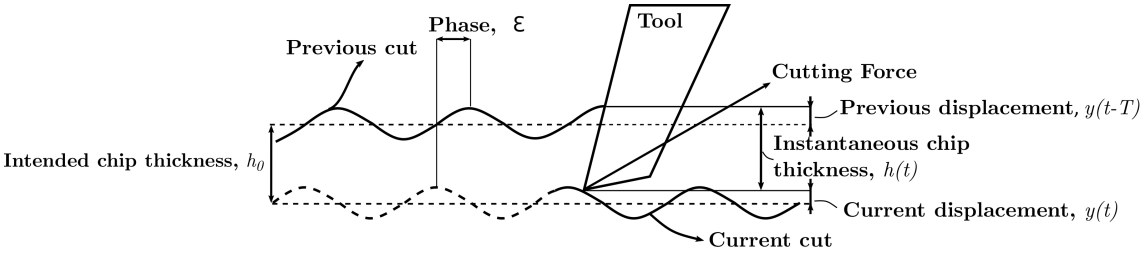

Figure 6: Depiction of a regenerative chatter mechanism

A chatter stability condition can be defined as the limiting depth of cut b_{lim}, which can be

simply expressed as [23]

$$b_{lim} = -\frac{1}{2K_s\Re\{H(j\omega)\}} \tag{7}$$

where K_s is specific cutting coefficient, which can be accepted as a constant term in this case and $Re\{H(j\omega)\}$ is the real part of the FRF of the system. The limiting depth of cut b_{lim} gives the stability boundary so the system becomes unstable beyond this value. The stability boundary can be increased by maximising the negative real part of the FRF when considering the depth of cut as a positive real number. Although Equation 6 is derived basing on a turning operation, it is approximately valid for a milling operation [22].

A milling operation can be reduced in a single-degree-of-freedom system so that Figure 3(a) can be used as the mathematical model of a machining operation controlled by a passive control device. Similar to the previous analysis, a parasitic mass can be added to the structure and the effects of the parasitic mass can be evaluated.

A similar analysis to the previous section was conducted. The primary mass, the natural frequency of the primary system and the damping ratio were taken as $M = 5\ kg$, $f_n = 200\ Hz$ and $\zeta_{primary} = 0.0035$. The milling operation parameters are presented in Table 2. The objective function for this case can be defined to maximise the negative minimum real part of the FRF of the system. Therefore, the objective function can be written as

$$max_{k,k_1,c,b}\left(min_{\omega}\big(\Re\{H_i(j\omega)\}\big)\right), i = 1, 2 \tag{8}$$

subject to $\Re\{H_i(j\omega)\} > 0$ and where $i = 1$, $i = 2$ and $i = 3$ represent for three mathematical models of no parasitic mass, the $icma$, and the $icmp$ cases, respectively.

Tool diameter	16 mm
Number of teeth	4
Radial immersion	4 mm
Tangential cutting stiffness	796.1 N/mm^2
Radial cutting stiffness	168.8 N/mm^2

Table 2: Milling simulation parameters

The optimal design parameters were found for mass ratio $\mu = 0.1$ and the case with no parasitic mass. The optimal inertance value for the case with no parasitic mass was almost the same as the previous case. Only 10% of the inertance value was added as the parasitic mass in the other two cases and the optimal design parameters were retuned. The optimal parameters are presented in Table 3. The stability boundaries are presented in Figures 7 and 8. The region under the stability boundary/curve represents a stable cutting condition. Thus, the higher curve means higher stability and hence improved productivity from the machining operation.

The stability lobe diagrams were compared with the stability diagram of the one controlled with a TMD whose optimal design parameters were obtained by Sims' tuning methodology [22]. It can be seen that the parasitic mass added into the configuration, whether the $icma$ or the $icmp$, removed the benefit of using an inerter as the stability boundary lowered to the level of one obtained with the TMD. The parasitic mass of $9.6\ g$ decreased the limiting depth of cut (the stability boundary) by 34.4% for the $icma$ and 17.6% for the $icmp$ configuration. After retuning the parameters considering the parasitic mass, the improvement obtained by using an inerter was regained as shown in Figure 8.

Configurations	m_p	$k\ [kN/m]$	$k_1\ [kN/m]$	$b\ [kg]$	$c\ [Ns/m]$
No parasitic mass	0	974.1	152.3	0.0956	69.2
$icma$	9.6 g	970.2	181.5	0.1048	82.7
$icmp$	9.6 g	996.6	157.6	0.0893	72.3

Table 3: Optimal design parameters obtained to increase machining chatter stability for $\mu = 0.1$.

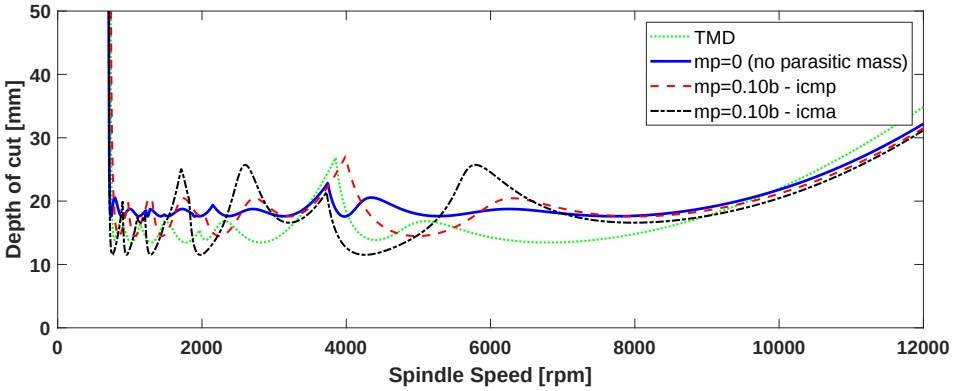

Figure 7: Stability lobe diagram obtained for three cases: No parasitic mass, the $icma$ and the $icmp$ by considering a parasitic mass of 10% of the optimal inertance value.

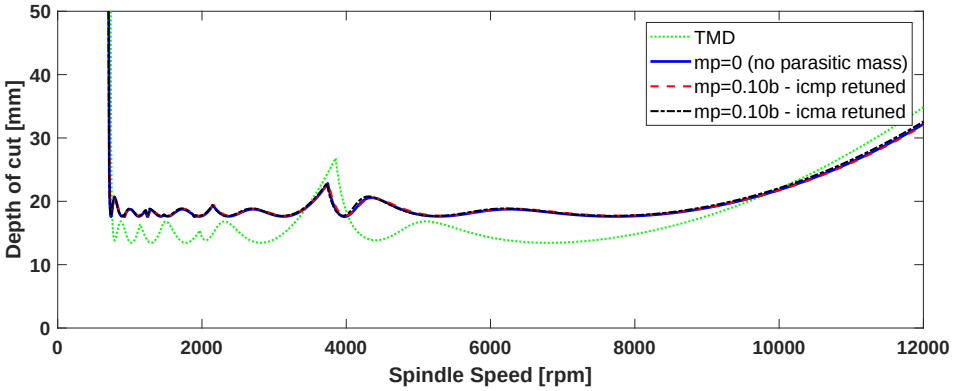

Figure 8: Stability lobe diagram after retuning the optimal parameters considering a parasitic mass of 10% of the inertance value.

6 Discussion

The results have shown that neglecting the mass of the inerter leads to a decrease in the vibration suppression and machining chatter stability performances since the optimal design parameters were obtained for the ideal condition, where the mass of the inerter is assumed as zero. For high ratios of the mass of the inerter to the inertance, the inertial effect of the mass of the inerter becomes insignificant as it is always coupled to the inertance (m_p+b) in the equations of motion. The structural mass of the inerter is generally designed to be small compared to the inertance but this cannot be always the case, especially for the applications where the modal mass of the primary system is small. It can be noted that the two cases for the location of the inerter the $icma$ and the $icmp$, had different behaviours. This should be considered in the design of the control device if the parasitic effect is inevitable.

Finally, it has seen that the improvement which is provided by using an inerter can be gained again by retuning the optimal parameters considering the parasitic mass. After the retuning the parameters, the results were slightly better than the result for an ideal inerter. The reason for this can be commented that the overall mass of the control device is increased by the parasitic mass. This can be seen as equal to the increase in the mass ratio. Therefore, it demonstrates slightly better performance.

7 Conclusion

The effects of the mass of the inerter on the performance of a system controlled by a inerter-based device was investigated for a generic vibration suppression scenario and also for the specific case of a machining dynamics problem. The mass of the inerter was assumed to be a lumped mass in the mathematical model and the FRFs were derived. Using the FRFs, the vibration suppression and machining stability performances of the system were examined. The result showed that if the ratio of the mass of the inertance to the inertance is not small enough, the mass of the inerter reduces the vibration performance of the system. However, the vibration performance was regained by retuning the optimal design parameters considering the parasitic mass.

REFERENCES

[1] H. Frahm, *Device for Damping Vibrations of Bodies*, 989,958 (1911).

[2] J. P. Den Hartog, Mechanical Vibrations, *McGraw-Hill, New York*, 1956.

[3] H. Kuroda, F. Arima, K. Baba, Y. Inoue, *Principles and characteristics of viscous damping devices (gyro-damper), the damping forces which are highly amplified by converting the axial movement to rotary one, 12th World Conference on Earthquake Engineering*, 2000.

[4] K. Saito, K. Yogo, Y. Sugimura, S. Nakaminami, K. Park, *Application of rotary inertia to displacement reduction for vibration control system, 13th World Conference on Earthquake Engineering*, 2004.

[5] M. C. Smith, *Synthesis of mechanical networks: the inerter, Proceedings of the 41st IEEE Conference on Decision and Control*, 2002.

[6] M. Z. Q. Chen, C. Papageorgiou, F. Scheibe, F. Wang, M. C. Smith The missing mechanical circuit element, *IEEE Circuits and Systems Magazine*, **9**, 10-26, 2009.

[7] F. Wang, M. Hong, T. Lin, Designing and testing a hydraulic inerter, *Journal of Mechanical Engineering Science*, **225**, 66-72, 2010.

[8] E. D. A. John, D. J. Wagg, Design and testing of a frictionless mechanical inerter device using living-hines, *Journal of the Franklin Institute*, **356** 7650-7668, 2019.

[9] M. C. Smith, F. Wang, Performance benefits in passive vehicle suspensions employing inerters, *Vehicle System Dynamics*, **42**, 235-257, 2004.

[10] Y. Hu, M. Q. Chen, Z. Shu, Passive vehicle suspensions employing inerters with multiple performance requirements, *Journal of Sound and Vibration*, **33**, 2212-2225, 2014.

[11] I. F. Lazar, S. A. Neild, D. J. Wagg, Using an inerter-based device for structural vibration suppression, *Earthquake Engineering and Structural Dynamics*, **43(8)**, 1129-1147, 2014.

[12] F. Wang, M. Hong, C. Chen, Building suspensions with inerters, *Proceedings IMechE, Journal of Mechanical Engineering Science*, **224**, 1605-1616, 2009.

[13] Y. Hu, J. Wang, M. Z. Q. Chen, Z. Li, Y. Sun, Load mitigation for a barge-type floating offshore wind turbine via inerter-based passive structural control, *Engineering Structures*, **177**, 198-209, 2018.

[14] Y. Li, J. Z. Jiang, S. Neild Inerter-based configurations for main-landing-gear shimmy suppression, *Journal of Aircraft*, **54(2)**, 684-693, 2017.

[15] F. Wang, C. Lee, R. Zheng, Benefits of the inerter in vibration suppression of a milling machine, *Journal of the Franklin Institute*, **356(14)**, 7689-7703, 2019.

[16] H. Dogan, N. D. Sims, D. J. Wagg, Investigation of the inerter-based dynamic vibration absorber for machining chatter suppression, *Journal of Physics: Conference Series*, **1264**, 2019.

[17] Y. Hu, M. Z. Q. Chen, Performance evaluation for inerter-based dynamic vibration absorbers, *International Journal of Mechanical Sciences*, **99**, 297-307, 2015.

[18] Y. Shen, L. Chen, X. Yang, D. Shi, J. Yang, Improved design of dynamics vibration absorber by using the inerter and its application in vehicle suspension, *Journal Sound and Vibration*, **361**, 148-158, 2016.

[19] E. Barredo, A. Blanco, J. Colin, V. M. Penagos, A. Abundez, L. G. Vela, V. Meza, R. H. Cruz, J. Mayen, Closed-form solutions for the optimal design of inerter-based dynamic vibration absorbers, *International Journal of Mechanical Sciences*, **144**, 41-53, 2018.

[20] F. Wang, M. Liao, B. Liao, W. Su, H. Chan, The performance improvements of train suspension systems with mechanical networks employing inerters, *Vehicle System Dynamics*, **47**, 805-830, 2009.

[21] A. K. Qin, P. N. Suganthan, *Self-adaptive differential evolution algorithm for numerical optimization, IEEE Congress on Evolutionary Computation*, 2005.

[22] N. D. Sims, Vibration absorbers for chatter suppression: a new analytical tuning methodology, *Journal of Sound and Vibration*, **301**, 592-607, 2007.

[23] T. L. Schmitz, K. S. Smith, Machining Dynamics: Frequency Respoonse to Improved Productivity, *Springer*, e-ISBN: 978-0-387-09645-2, 2009.

[24] Y. Altintas, Manufacturing Automation: Metal Cutting Mechanics, Machine Tool Vibration, and CNC Design, *Cambridge University Press*, ISBN: 978-0-521-17247-9, 2012.